Broadband Cloaking in Stratified Seas

Mohammad-Reza Alam[1]

[1]Department of Mechanical Engineering, University of California, Berkeley, California 94720, USA

(Received 13 September 2011; published 23 February 2012)

Here we show that floating objects in stratified fluids can be cloaked against broadband incident waves by properly architecting the bottom corrugations. The presented invisibility cloaking of gravity waves is achieved utilizing a nonlinear resonance concept that occurs between surface and internal waves mediated by the bottom topography. Our cloak bends wave rays from the surface into the body of the fluid. Wave rays then pass underneath the floating object and may be recovered back to the free surface at the downstream bearing no trace of diffraction or scattering. The cloak is the proper architecture of bottom corrugations only, and hence is surface noninvasive. The presented scheme is a nonlinear alternative to the transformation-based cloaking, but in the context of dispersive waves.

DOI: 10.1103/PhysRevLett.108.084502 PACS numbers: 47.35.Bb, 47.11.Kb, 47.20.Ma, 47.55.Hd

The density of water in an ocean or a sea is typically not constant. The variation of density is due to, mainly, variations of temperature and salinity. Solar radiation heats up the upper layer of the water, and the flow of rivers and the melting of ice lower the water density near the surface. Over time these effects add up to form a stable density stratification with the lighter fluid on top and the denser fluid below it. Stratified waters, besides regular surface waves, admit the so-called internal waves, which are gravity waves that propagate within the body of the water [1].

Field observations have reported ubiquitously nonuniform vertical gradient of stratification in the oceans: water density is nearly constant in an upper layer and then jumps, over a (relatively) thin horizontal plane of sudden density change—the so-called thermocline—, to a denser lower layer fluid. Density stays almost constant below the thermocline to the ocean floor (e.g., [2]). Therefore, for ocean scenarios a two-layer model, with the density of each layer constant within the layer, is plausible and widely used. If a two-layer density stratification assumption is employed, internal waves are restricted to propagate on the thermocline only. These waves, sometimes also called interfacial waves, are widely observed in the oceans, seas, and lakes [1,3–5].

Here we present the formation of a resonance between surface waves and interfacial waves caused by the physics of inhomogeneity (stratification) of ocean waters, the dispersive nature of gravity waves, and the nonlinearity of equations governing the motion of a fluid. This resonance can be utilized to create a cloak of invisibility about ocean objects against incident surface waves. The invisibility cloak of water waves must detour wave rays about the object as if the object does not exist. Incident waves, as a result, must be able to propagate forward without interruption, i.e., with no trace of diffraction.

Specifically, consider a monochromatic surface wave train with wavelength $\lambda_s = 2\pi/k_s$ arriving from $x = -\infty$. Our objective is to create a cloaked buffer zone about $x = 0$ where our hypothetical floating object resides. We will show that a series of properly architected bottom undulations can effectively transfer the energy from the incident surface wave to internal waves, i.e., from the surface to within the body of water, and vice versa. Internal waves can later be fully recovered back to the surface at downstream. These recovered surface waves in the downstream carry no trace of the object because they have bypassed the encounter via nonlinear interaction with our bottom-mounted cloak; hence, invisibility is achieved.

In contrast to electromagnetic and acoustic cloaking based on coordinate transformation [6] and the use of metamaterials [7–12], where so far the invisibility is limited to a single frequency (radar and microwave), and also perfect invisibility is impossible [8,13], we prove theoretically that in our scheme a complete cloaking is achievable. We also present computational evidence of monochromatic and broadband cloaking. We note that, specific to ocean applications, the cloaking is more important in *protecting* ocean objects against powerful incoming waves than making their trace invisible.

Consider a two-layer density stratified fluid with ρ_u, ρ_ℓ and h_u, h_ℓ, respectively, upper and lower layer densities and depths (Fig. 1). In each layer, we assume that the fluid is homogeneous, incompressible, immiscible and inviscid, and we neglect the effects of surface tension. Under these assumptions a two-layer fluid admits two types of propagating waves associated with a given frequency ω (see Supplemental Material SI for the governing equation [14]): a surface wave with the wave number k_s and an interfacial wave with the wave number $k_i \gg k_s$, where k_s, k_i are solutions of the so-called dispersion relation

$$\begin{aligned}\mathcal{D}(k,\omega) \equiv\ & \omega^4(\mathcal{R} + \coth kh_u \coth kh_\ell) \\ & - \omega^2 gk(\coth kh_u + \coth kh_\ell) \\ & + g^2k^2(1-\mathcal{R}) = 0, \end{aligned} \tag{1}$$

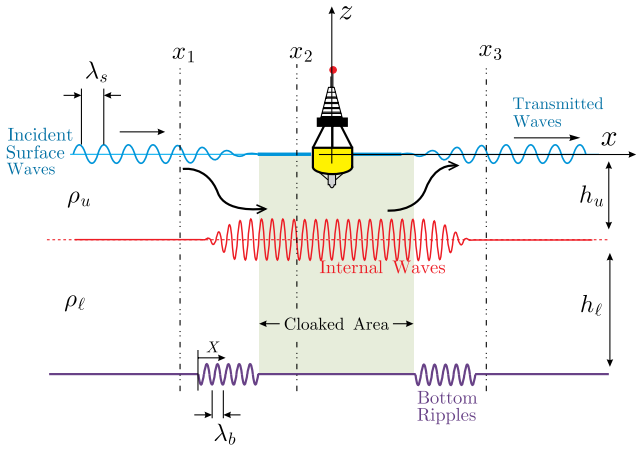

FIG. 1 (color online). Schematic representation of cloaking mechanism in a two-layer density stratified fluid. An incident wave of wave number $k_s = 2\pi/\lambda_s$ gives its energy to an interfacial wave k_i, of the same frequency, over a patch of bottom ripples $k_b = k_i - k_s$ hence leaving a cloaked buffer zone of invisibility. The interfacial wave can be recovered at the downstream ($x > 0$) by the same mechanism.

in which $\mathcal{R} = \rho_u/\rho_\ell$ is the density ratio and g is gravity acceleration.

Bottom roughnesses scatter both surface and interfacial waves (e.g., [15]). If bottom irregularities follow a specific pattern then scattered waves may constructively interfere to form one single ray with a specific wavelength. This phenomenon is called Bragg resonance of water waves named after its close cousin phenomenon in solid state physics of crystals [16]. Contrary to Bragg reflection from crystals which is a linear phenomenon, Bragg resonance of water waves is a nonlinear phenomenon. In perturbation expansion of governing equations in terms of a small parameter (usually wave steepness ka, k being the wave number and a the amplitude of wave) Bragg resonance occurs at the second order (class I), third order (class II and III), and higher orders of nonlinearities [17,18].

In a homogeneous fluid if bottom has periodic undulations with the wavelength equal to half of the wavelength of the incident wave, then incident waves will be (partially) reflected [17–21]. The reflection coefficient (ratio of amplitude of reflected wave to the amplitude of incident wave) is a function of length of the patch of undulations and asymptotically approaches one as the extent of the patch stretches to infinity.

For a two-layer density stratified fluid we have recently shown [22,23] that at the leading (second) order nonlinearity six scenarios of Bragg resonance is possible. If we have an incident surface wave (k_s), then depending on bottom properties the resonant wave may be a reflected surface wave, a reflected interfacial wave or a transmitted interfacial wave. If the incident wave is an interfacial wave, then the resonant wave may be a reflected interfacial wave, a reflected surface wave or a transmitted surface wave.

For cloaking purposes we are interested in cases where the resonant wave is a transmitted wave. Specifically, consider an incident surface wave of wave number k_s. Now, if bottom undulations wave number k_b satisfies the resonance condition $k_b = k_i - k_s$, then over the patch of bottom ripples the surface wave gives its energy to the interfacial wave (see left side of Fig. 1). If amplitude of incident surface wave and resonant interfacial wave is given, respectively, by $A_s(X)$ and $A_i(X)$ where X is horizontal dimension measured from the beginning of the ripple patch, then using multiple scales techniques it can be shown that [22]:

$$A_s(X) = \alpha \cos(\kappa X), \qquad A_i(X) = \beta \sin(\kappa X), \tag{2}$$

where α, β and κ are functions of ocean parameters (see Supplemental Material SII [14] for expressions of these coefficients). If the length of the bottom patch is exactly $X_b = \pi/(2\kappa)$ then Eq. (2) predicts that the amplitude of incident wave reaches exactly zero at the end of the patch. Physically speaking, at this distance surface wave energy has been completely transferred to the interface. The same bottom patch can in reverse transfer the energy of an incident interfacial wave to a resonant surface wave and is used on the right hand side of the ocean object to recover the surface wave (Fig. 1). Therefore, theoretically, a perfect cloaking is achieved.

If the incident wave train is polychromatic, i.e., with many components forming a spectrum of waves, leading order cloaking is achieved by the superposition of proper bottom undulations for each of incident wave components. This, usually, does not require additional space, but just a polychromatic bottom undulations, hence can be readily achieved.

Theoretical analysis of broadband cloaking is, however, very limited. Usually when more than just a few wave components interact simultaneously it is algebraically tedious—if not impossible—to track their interactions. This fact becomes more highlighted when we notice that for an accurate prediction of the evolution of a spectrum of waves over a patch of bottom ripples several nonlinear interaction scenarios including, but not limited to, sub and superharmonic generations [24,25], triad and quartet resonance between waves [26–28] and high-order Bragg resonances [22,23] must be taken into account. To address the problem of many (typically $N = O(10^4)$] waves interacting and to consider an arbitrary order of nonlinearity [typically $M = O(10)$ in terms of perturbation expansion) we have recently extended a direct simulation scheme based on a high-order spectral method (HOS), originally derived to study nonlinear wave-wave [29] and wave-bottom [17] interactions, to a two-layer density stratified fluid with finite-depth upper and lower layers ([22], where extensive convergence tests and validations with experimental data are also provided). Here we use HOS to, besides validating our

theoretical predictions, study the initial-value problem of surface waves (monochromatic and broadband) impinging upon our cloak of invisibility.

We first consider a monocrhomatic incident surface wave of wave number and frequency $k_sH = 0.34$ and $\omega\sqrt{H/g} = 0.36$, with $H = h_u + h_\ell$, in a two-layer density stratified fluid of $\mathcal{R} = 0.95$ and $h_u/H = 1/2$ (relevance of chosen values to real life applications are discussed in the Supplemental Material, SIII). At $t/T = 0$ it is assumed that the water surface is calm and a train of waves arrives from $x = -\infty$ to the domain of our interest $-70 < k_sx < 70$. A bottom patch of dimensionless wave number $k_bH = k_iH - k_sH = 4.86$ (where k_i is the interfacial wave solution of (1) for frequency ω) forms a resonance between k_s, k_i. From multiple scales analysis results (2) it is seen that if $n_b = k_b/(4\kappa)$ number of bottom undulations are placed on the seafloor all the energy of k_s is transformed to k_i. Comparison of theoretical results (2) (dashed lines) with direct simulation of initial-value problem of this example after a steady state is reached (solid lines) are presented in Fig. 2. For direct simulation we have chosen $N = 2048$, $M = 3$, $T/\delta t = 64$ for which the computation is converged. Figure 2 shows a good agreement between analytical results and direct computations. The cloaked zone is clearly formed in the area of $-6 < k_sx < 6$ where surface activity is minimal.

To better assess the transient response of our cloak as it encounters the incident wave and until it reaches a steady state, Fig. 3 shows the amplitude of waves predicted by solving the initial-value problem using our spectral-based direct simulation scheme. Amplitude of surface waves at three stations of x_1, x_2, and x_3 (cf. Fig. 1), respectively, upstream, in the cloaked zone and downstream, are plotted in Figs. 3(a)–3(c). In each figure the amplitude of waves in the presence and in the absence of the cloak is presented. In upstream [Fig. 3(a)] and in the absence of the cloak the monochromatic wave train marches forward without any interruption; hence, no variation in the amplitude is expected. If the cloak exists Fig. 3(a) shows again no variation in the upstream amplitude which implies that the cloak does not reflect any waves. In the cloaked zone however, the surface amplitude is greatly reduced [Fig. 3(b)]. The observed nonzero surface activity (i.e., the error) is mainly due to the image of the interfacial waves on the surface. Because of its short wavelength this image is easily detectable in Fig. 2 on the surface of water in the cloaked zone. Note that these short waves are not seen outside the cloak where interfacial wave amplitude is small. Finally, Fig. 3(c) shows the downstream spectrum. With the cloak and after a transition period is passed, the downstream spectrum approaches that of the upstream. The three Figs. 3(a)–3(c) show the performance of our bottom-mounted cloak in creating a buffer zone of

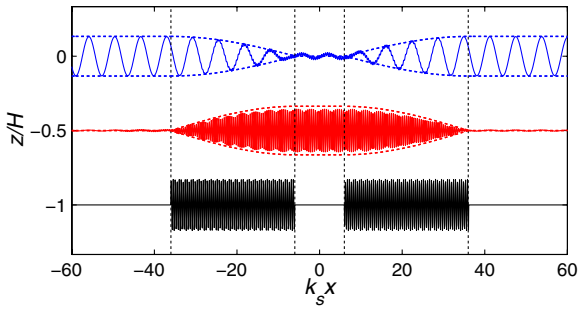

FIG. 2 (color online). Cloaking against a monochromatic incident surface wave. Plotted results are analytical solution based on multiple scales theory (2) (dashed line), and direct simulation of HOS (solid line). A surface wave $k_sH = 0.34$ enters from $x = -\infty$ and exchanges its energy to the interface as it travels over the first bottom patch ($-36 < k_sx < -6$). In a reverse process the interfacial wave gives back its energy to the surface as it travels over the second patch of bottom ripples ($6 < k_sx < 36$). As a result, a cloaked buffer zone ($-6 < k_sx < 6$) is formed where surface activity is very small. Surface and interfacial elevations are magnified by factors of, respectively, 1000 and 50 for easier realization.

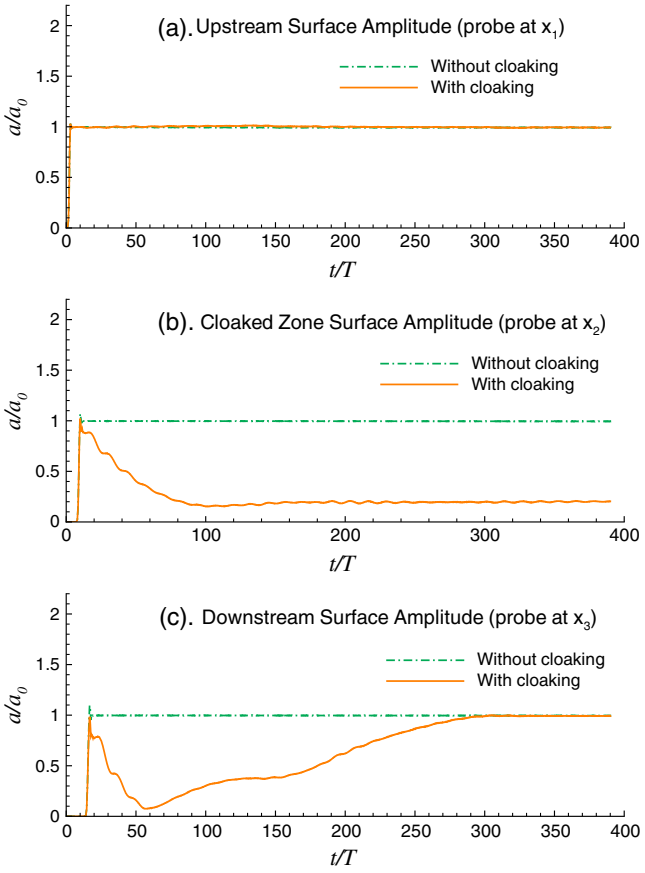

FIG. 3 (color online). Time history of evolution of surface wave amplitude obtained from direct simulation at (a) $k_sx_1 = -40$, (b) $k_sx_2 = 0$, and (c) $k_sx_3 = 40$ (cf. Fig. 1). Results plotted are the upstream (incident) wave in the absence of bottom undulations given for the reference (dash-dotted line), and the surface wave amplitude in the presence of cloaking (solid line).

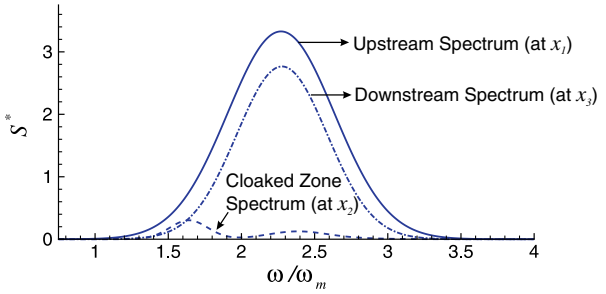

FIG. 4 (color online). Cloaking against a spectrum of waves. Plotted curves are the upstream (incident) wave spectrum (solid line), downstream spectrum (dash-dotted line), and spectrum in the cloaked zone (dashed line). $\int S^* d\omega = \sum_{i=1,5} 1/2(a_i/a_m)^2$, with a_i amplitude of each individual wave normalized by a_m the amplitude of the median wave.

invisibility, and also in recovering the wave to the surface with the minimal loss.

For a broadband spectrum of incident waves, leading order cloaking is achieved by the superposition of bottom profiles required by each of wave components in the spectrum. Consider a broadband Gaussian spectrum of incident waves (Fig. 4, solid line) arriving to the location of our hypothetical floating object to be cloaked. For direct simulation purposes, we discretize this spectrum into five individual waves and superimpose the five bottom wave number on top of each other to form a polychromatic patch of corrugations (details of numerical simulation is provided in the Supplemental Material SIV [14]). Figure 4 presents the result of direct simulation of an incident broadband spectrum as it travels over the bottom cloak. After a steady state is reached the cloaked zone (dash line) experiences negligible wave activity, only $\sim$%5 of incident wave energy. The downstream spectrum (dash-dotted) is close to the incident spectrum recovering more than %70 of incident wave energy. Besides the source of error already discussed for monochromatic cloaking, in the case of a broadband spectrum nonlinear interactions between waves within the spectrum are also affecting the performance of the cloaking. A smart design of an efficient (higher-order) broadband cloak requires care to avoid unwanted resonances.

Results obtained here are also valid in the presence of a floating object. An example of cloaking in the presence of a heaving disturbance is discussed in the Supplemental Material SV [14]. If the bottom is not flat (e.g., sloped) then ripples can be adjusted in order to retain the high performance of the cloaking scheme (see Supplemental Material SVI [14]). It is to be noted that the demonstrated scheme for unidirectional cloaking can be extended to omnidirectional cloaking by the use of radial Bragg resonance (i.e., concentric circular bottom undulations). Nevertheless, in the context of ocean waves, due to the refraction of waves in (relatively) shallower waters, this is of less importance and hence is not pursued here.

In summary, we have demonstrated that floating objects in stratified fluids can be cloaked against broadband incident waves by properly architecting the bottom corrugations. The concept behind the presented scheme is based on nonlinear resonance of surface and interfacial waves with the bottom topography and is obtained due to the dispersive nature of gravity waves. Perfect cloaking against monochromatic waves can theoretically be achieved and was further investigated via a direct high-order spectral scheme. Broadband cloaking was also elucidated and its performance is discussed. The cloak introduced here is the alignment of bottom corrugations only, and therefore is surface noninvasive. Cloaking in seas by bottom modifications may play a role in protecting near shore or offshore structures (buoys) and in creating shelter for fishermen during storms. In reverse it can result in disappearance and appearance of surface waves in areas where sandbars (or any other appreciable bottom variations) exist.

Bragg scattering or resonance, although may differ in details, but is a common concept in solid state physics [30,31], optics (e.g., [32]), acoustics (e.g., [33]) and hydrodynamics [17–19]. The idea demonstrated here may have similar implications in any system admitting Bragg resonance and if its medium can be freely architected.

I would like to thank Dr. Y. Liu and Dr. R. Karimi for careful reading of the manuscript and valuable comments. The support from the American Bureau of Shipping is greatly acknowledged.

[1] C. Garrett and W. Munk, Annu. Rev. Fluid Mech. **11**, 339 (1979).
[2] D. Sigman, S. Jaccard, and G. Haug, Nature (London) **428**, 59 (2004).
[3] J. T. Holt and S. A. Thorpe, Deep-Sea Research, Part I **44**, 2087 (1997).
[4] W. Choi and R. Camassa, Phys. Rev. Lett. **77**, 1759 (1996).
[5] L. Boegman, J. Imberger, G. N. Ivey, J. P. Antenucci, and A. Hogg, Limnol. Oceanogr. **48**, 895 (2003).
[6] A. Ward and J. Pendry, J. Mod. Opt. **43**, 773 (1996).
[7] J. B. Pendry, D. Schurig, and D. R. Smith, Science **312**, 1780 (2006).
[8] U. Leonhardt, Science **312**, 1777 (2006).
[9] S. a. Cummer, B.-I. Popa, D. Schurig, and D. R. Smith, Phys. Rev. E **74**, 1 (2006).
[10] D. Schurig, J. J. Mock, B. J. Justice, S. A. Cummer, J. B. Pendry, A. F. Starr, and D. R. Smith, Science **314**, 977 (2006).
[11] Y. Urzhumov and D. Smith, Phys. Rev. Lett. **107**, 074501 (2011).
[12] M. Farhat, S. Enoch, S. Guenneau, and a. Movchan, Phys. Rev. Lett. **101**, 134501 (2008).
[13] P. Yao, Z. Liang, and X. Jiang, Appl. Phys. Lett. **92**, 031111 (2008).
[14] See Supplemental Material at http://link.aps.org/supplemental/10.1103/PhysRevLett.108.084502 for details of governing equations, explicit forms of coefficients

presented in the main text, discussion on the relevance to the real world applications, and two illustrative examples that supplement the main text.

[15] M.-R. Alam and C. C. Mei, J. Fluid Mech. **587**, 73 (2007).
[16] W. H. Bragg and W. L. Bragg, Proc. R. Soc. A **88**, 428 (1913).
[17] Y. Liu and D. K.-P. P. Yue, J. Fluid Mech. **356**, 297 (1998).
[18] M.-R. Alam, Y. Liu, and D. K. P. Yue, J. Fluid Mech. **643**, 437 (2010).
[19] C. C. Mei, J. Fluid Mech. **152**, 315 (1985).
[20] A. Davies, Dynamics of Atmospheres and Oceans **6**, 207 (1982).
[21] X. Hu and C. Chan, Phys. Rev. Lett. **95**, 154501 (2005).
[22] M.-R. Alam, Y. Liu, and D. K. P. Yue, J. Fluid Mech. **624**, 191 (2009).
[23] M.-R. Alam, Y. Liu, and D. K. P. Yue, J. Fluid Mech. **624**, 225 (2009).
[24] P. J. Bryant, J. Fluid Mech. **59**, 625 (1973).
[25] C. Mei and U. Unluata, in *Waves on Beaches and Resulting Sediment Transport* (Academic Press, New York, NY, 1971), p. 181.
[26] F. K. Ball, J. Fluid Mech. **19**, 465 (1964).
[27] F. Wen, Phys. Fluids **7**, 1915 (1995).
[28] M.-R. Alam, J. Fluid Mech. **691**, 267 (2012).
[29] D. G. Dommermuth and D. K. P. Yue, J. Fluid Mech. **184**, 267 (1987).
[30] P. J. Martin, B. G. Oldaker, A. H. Miklich, and D. E. Pritchard, Phys. Rev. Lett. **60**, 515 (1988).
[31] E. Fermi and L. Marshall, Phys. Rev. **71**, 666 (1947).
[32] G. Kryuchkyan and K. Hatsagortsyan, Phys. Rev. Lett. **107**, 053604 (2011).
[33] L. Feng, X.-P. Liu, M.-H. Lu, Y.-B. Chen, Y.-F. Chen, Y.-W. Mao, J. Zi, Y.-Y. Zhu, S.-N. Zhu, and N.-B. Ming, Phys. Rev. Lett. **96**, 014301 (2006).